

Supplementary Information for

A Microfluidic Method for Dopamine Uptake Measurements in Dopaminergic Neurons

Yue Yu,^{1,2} Mohtashim H. Shamsi,^{2,3†} Dimitar L. Krastev,⁴ Michael D. M. Dryden,³ Yen Leung,²
Aaron R. Wheeler^{1, 2,3*}

¹ Institute for Biomaterials and Biomedical Engineering, University of Toronto, 164 College St, Toronto, ON, M5s 3G9, Canada

² Donnelly Centre for Cellular and Biomolecular Research, 160 College St., Toronto, ON, M5S 3E1, Canada

³ Department of Chemistry, University of Toronto, 80 St Georg St., Toronto, ON, M5S 3H6, Canada

⁴ Department of Human Biology, University of Toronto, 300 Huron Street, Toronto, ON, M5S 3J6, Canada

† Current Address:

Department of Chemistry and Biochemistry, Southern Illinois University at Carbondale, 1245 Lincoln drive, Carbondale, IL, 62901, USA

* Corresponding Author:

Email: aaron.wheeler@utoronto.ca

Tel: 416-946-3864

Fax: 416-946-3865

Simulation of Diffusion Onto Electrodes

COMSOL Multiphysics (COMSOL, Inc., MA, USA) was used on licence through CMC Microsystems (Kingston, ON). The Transport and Diluted Species module was chosen for the simulation, with an isotropic diffusion profile and a diffusion coefficient of 8×10^{-7} cm²/s. A quarter-cell (90° pie, Fig S1a-d) was created by subtracting two rectangular ($2 \times 1 \times 0.2$ mm) blocks from a cylinder ($r = 1$ mm, $h = 0.2$ mm). The two rectangular side faces of the quarter-cell were set to the 'symmetry' parameter. A work plane was created on the bottom face of the quarter cell and populated with a secondary shape matching the desired electrode geometry (round, line, cross, star, with dimensions listed in the main text). The mesh was calibrated for general physics with maximum element size = 0.01 mm, minimum element size = 10^{-5} mm, maximum element growth rate = 1.3, resolution of curvature = 0.2, and resolution of narrow regions = 1. A time dependent study was applied to solve for $\text{Cl}_2\text{Ru}(\text{Phen}_3)^{2+}$ concentration with start = 0 s, end = 10 s, and time step = 0.1 s. At start, the electrode surface area was defined to have $[\text{Cl}_2\text{Ru}(\text{Phen}_3)^{2+}] = 0$ M [to simulate the complete oxidation of $\text{Cl}_2\text{Ru}(\text{Phen}_3)^{2+}$], while the entire volume of the cell and all other surfaces were defined to have $[\text{Cl}_2\text{Ru}(\text{Phen}_3)^{2+}] = 200$ μM . Images (Fig. S1e-h) were generated using the build-in results section of COMSOL. The total flux of analyte onto each electrode was integrated from start to end and is plotted in Figure 2c in the main text.

SH-SY5Y Neurite Growth Progression

Neuron seeding, culture, and differentiation on DMF devices was carried out as described in the main text. After treatment with differentiation agents (RA or TPA) for differentiated cells or vehicle (cell culture medium) for non-differentiated cells on days 0, 3, and 6, the top plates were fixed in 4% paraformaldehyde, stained for β 3-tubulin and mitochondria, and imaged (Fig. S2a-d) as described in the main text. At least 5 images were evaluated for each condition using the NeuronJ plugin of ImageJ as described previously (Meijering et al. *Cytometry Part A*, 2004, **58A**, 167-176). Briefly, in each image, 15 randomly selected cells were chosen for measurement. For each cell, the length of the longest neurite was measured from the base of the axon hillock to the tip of the growth cone (Fig. S2e).

Wash efficiency

DMF devices bearing EM-top plates (with star-shaped WEs and cell culture sites) were formed and used as described in the main text. As noted in the main text, cell culture sites (i.e., the 2 mm dia. circular apertures free of Teflon AF upon which cells adhere and grow) support the phenomenon of passive dispensing—that is, when two or more 600 nL unit droplets are driven across a cell culture site, a 470 nL virtual microwell (VM) is left behind. Although not emphasized in the main text, each electrochemical sensor (comprising one WE and one CE/RE) is also embedded in a 2 mm dia. hydrophilic liftoff area, and thus also supports passive dispensing to form 470 nL VMs. This feature was used to evaluate the transfer efficiency for analyte collection from a VM.

Transfer efficiency was determined using two different analytes: 1 μ M 1:1 potassium hexacyanoferrate(II):potassium hexacyanoferrate(III) (FF), and dopamine (DA). First, amperometric calibration curves for both analytes were generated on-chip by performing cyclic voltammetry on analyte-containing VMs (470 nL each, containing 1 mM to 100 nM FF in 1 \times

PBS, or 1 μM to 10 nM DA in $1\times$ PBS). Five CVs were collected for each concentration (FF: 0.25 V s^{-1} , from -1.2 V to 1.2 V; DA: 0.1 V s^{-1} , from -0.9 V to 0.9 V), discarding the first two and keeping the final three for analysis. The average peak cathodic currents (FF: 0.6 V; DA: 0.72 V) were plotted as a function of concentration and fitted with linear least squares regressions. Second, 470 nL VMs were formed over each sensor again, each containing 1 mM FF or 1 μM DA. In each test, a unit droplet (600 nL) of $1\times$ PBS buffer (containing no FF or DA) was driven across the VM, collecting most of the analyte, leaving behind a new VM bearing a small amount of residual analyte. Each VM was interrogated by cyclic voltammetry (as above) before and after the PBS droplet transfer. The average peak cathodic currents (FF: 0.6 V; DA: 0.72) before and after transfer were used with the calibration curves described above to estimate the amount of analyte remaining in the VM. The results are summarized in Figure S3.

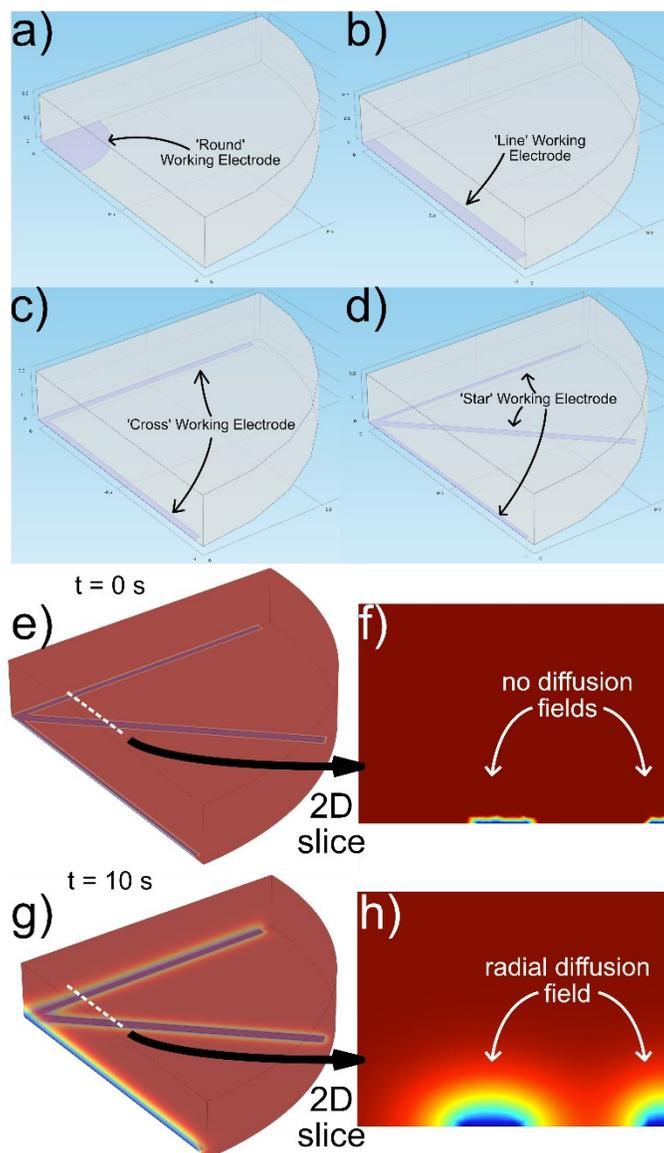


Figure S1 – COMSOL model of diffusion on different working electrode (WE) geometries. a-d) Schemes for the quarter-cell models ($r = 1 \text{ mm}$) for each WE geometry: round, line, cross, star. In each model, the working electrode shape is shown in blue. In each simulation, at start, the electrode area was set to $0 \text{ M Cl}_2\text{Ru(Phen}_3\text{)}^{2+}$ while the remaining volume was set to $200 \mu\text{M}$. Frames illustrating the start (time = 0 s) and end (time = 10 s) of the simulation are shown for the star-shaped WE as a heat map with red = $200 \mu\text{M}$ and blue = 0 M in e-f) and g-h), respectively.

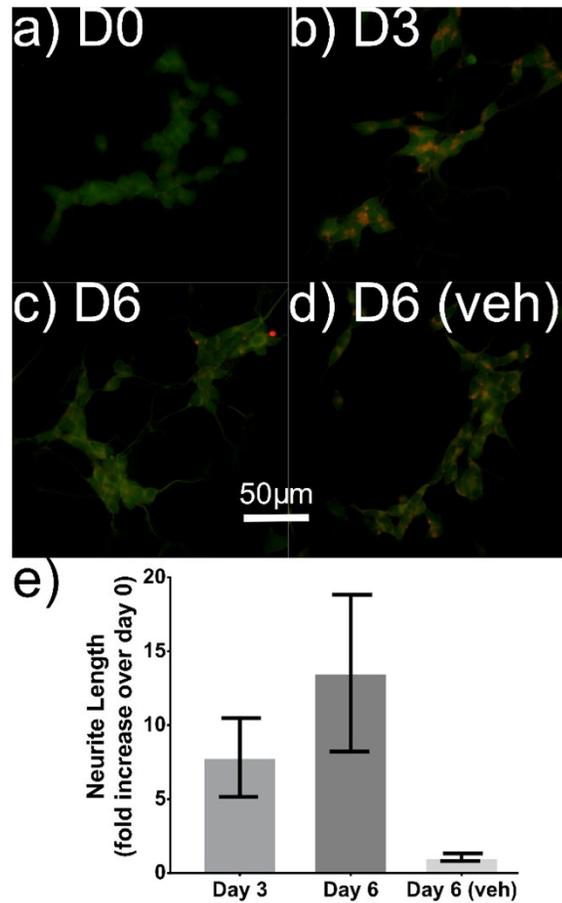


Figure S2 – SH-SY5Y neurite growth progression. Representative fluorescent micrographs (40 \times mag.) of SH-SY5Y neurons on a) day 0, b) day 3 (after 3 days with RA), c) day 6 (after 3 additional days with TPA), and d) day 6 (after 6 days with vehicle). Neurons were stained for β III-tubulin (green), and mitochondria (red). **Scale bar is 50 μ m.** e) Bar graph indicating the average fold-change of the main neurite length of neurons at day 3 and 6 compared to day 0. Error bars represent ± 1 standard deviation (S.D.) for $n = 60$. Neurite length increases with incubation in RA; growing 8-fold by day 3, and additionally with incubation in TPA up to 15-fold by day 6. Day 6 SH-SY5Y cells treated with vehicle exhibit neurite lengths similar to day 0 immature SH-SY5Y cells.

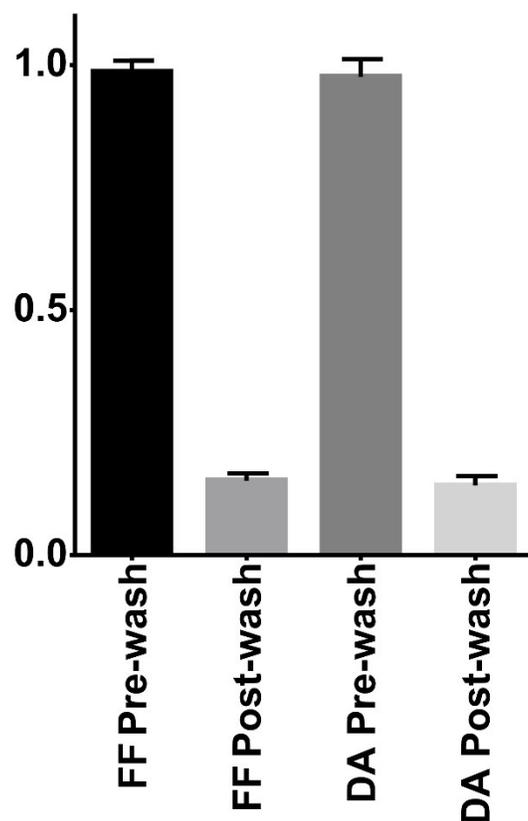


Figure S3 – Determination of analyte transfer efficiency for virtual microwells. Each bar indicates the amount of 1 mM 1:1 potassium hexacyanoferrate(II):potassium hexacyanoferrate(III) (FF) or 1 μ M dopamine (DA) measured in 470 nL virtual microwells (VMs) before (left) and after (right) each VM is “washed” by passing a unit droplet (600 nL) of PBS (containing no FF or DA) across the sensor. Error bars represent 1 standard deviation (S.D.) for $n = 10$. The post-wash data shows that $15\% \pm 3\%$ of the FF solution and $14\% \pm 2\%$ of the DA solution remains in the virtual microwell after a single transfer.